Transgenic Res (2007) 16:193–201
DOI 10.1007/s11248-006-9056-9

ORIGINAL PAPER

Effects of FVB/NJ and C57Bl/6J strain backgrounds on mammary tumor phenotype in inducible nitric oxide synthase deficient mice

Sarah A. Davie · Jeannie E. Maglione · Cathyryne K. Manner · Dmitri Young · Robert D. Cardiff · Carol L. MacLeod · Lesley G. Ellies

Received: 28 August 2006 / Accepted: 13 November 2006 / Published online: 6 January 2007

Abstract The ability to genetically manipulate mice has led to rapid progress in our understanding of the roles of different gene products in human disease. Transgenic mice have often been created in the FVB/NJ (FVB) strain due to its high fecundity, while gene-targeted mice have been developed in the 129/SvJ-C57Bl/6J strains due to the capacity of 129/SvJ embryonic stem cells to facilitate germline transmission. Gene-targeted mice are commonly backcrossed into the C57Bl/6J (B6) background for comparison with existing data. Genetic modifiers have been shown to modulate mammary tumor latency in mouse models of breast cancer and it is commonly known that the FVB strain is susceptible to mammary tumors while the B6 strain is more resistant. Since gene-targeted mice in the B6 background are frequently bred into the polyomavirus middle T (PyMT) mouse model of breast cancer in the FVB strain, we have sought to understand the impact of the different genetic backgrounds on the resulting phenotype. We bred mice deficient in the inducible nitric oxide synthase (iNOS) until they were congenic in the PyMT model in the FVB and B6 strains. Our results reveal that the large difference in mean tumor latencies in the two backgrounds of 53 and 92 days respectively affect the ability to discern smaller differences in latency due to the Nos2 genetic mutation. Furthermore, the longer latency in the B6 strain enables a more detailed analysis of tumor formation indicating that individual tumor development is not stoichastic, but is initiated in the #1 glands and proceeds in early and late phases. NO production affects tumors that develop early suggesting an association of iNOS-induced NO with a more aggressive tumor phenotype, consistent with human clinical data positively correlating iNOS expression with breast cancer progression. An examination of lung metastases, which are significantly reduced in PyMT/iNOS$^{-/-}$ mice compared with PyMT/iNOS$^{+/+}$ mice only in the B6 background, is concordant with these findings. Our data suggest that PyMT in the B6 background provides a useful model for the study of inflammation-induced breast cancer.

Keywords FVB/NJ · C57Bl/6J · Strain · iNOS · Breast · Cancer · Polyomavirus middle T antigen · Mouse

S. A. Davie · J. E. Maglione · C. K. Manner · D. Young · C. L. MacLeod · L. G. Ellies (✉)
Moores UCSD Cancer Center, Department of Medicine, University of California, San Diego, 9500 Gilman Drive, La Jolla, San Diego, CA 92093-0063, USA
e-mail: lellies@ucsd.edu

R. D. Cardiff
Center for Comparative Medicine, University of California, Davis, Davis, CA 95616, USA

Abbreviations
(iNOS) inducible nitric oxide synthase
(PyMT) polyomavirus middle T antigen

Introduction

Transgenic mouse models that develop spontaneous mammary adenocarcinomas have proven valuable in revealing molecular mechanisms underlying tumorigenesis and metastasis (Cardiff 2003; Fargiano et al. 2003). Models target specific pathways depending on the transgene being expressed under the control of the mouse mammary tumor virus long terminal repeat (MMTV-LTR) or whey acid protein (WAP) mammary gland promoters and thereby replicate genetic defects in subsets of human tumors (Cardiff and Wellings 1999; Rosner et al. 2002). Molecules from pathways known to be important in the pathogenesis of human breast cancer such as the Wnt, Ras and ErbB2/Neu pathways have been utilized, however few spontaneous mammary tumor model systems develop metastasis, a crucial aspect of cancer progression.

As demonstrated by gene expression analysis (Ma et al. 2003), the polyomavirus middle T (PyMT) model in the FVB/N (FVB) background activates the same signaling pathways as erbB2, an oncogene amplified or overexpressed in approximately 30% of human breast cancers. The model has been particularly useful for genetic studies due to its short tumor latency and high incidence of pulmonary metastasis (Guy et al. 1992). These features have enabled global expression profiling of PyMT tumors from different genetic backgrounds to identify signatures of tumor virulence (Qiu et al. 2004) that are consistent with a gene set predictive of metastasis in human tumors (Ramaswamy et al. 2003). Hence, the model has been used effectively to dissect early and late stages of mammary tumor development (Guy et al. 1994; Lin et al. 2001; Webster et al. 1998; Williams et al. 2004). In women with breast cancers involving this pathway, the course of the disease varies widely. One powerful means to understand that variability is to identify useful animal models. The PyMT breast cancer model can be used in genetic crossing experiments to identify loci having modifier effects on either tumorigenesis or metastasis (Le Voyer et al. 2000). An understanding of the genetic polymorphisms underlying these effects is important in the study of human cancer as genetic variability affects host-tumor interactions in numerous ways and is an important factor in the response to therapy.

Widely varied tumor responses to polyoma virus infection among different inbred strains of mice have been well documented (Freund et al. 1992; Gross 1983). Much of this difference can be attributed to the major histocompatibility complex (MHC) which results in immunologically mediated resistance associated with an H-2^b haplotype such as in C57Bl strains (Law et al. 1967; Ting and Law 1965). Other inbred strains, notably those with the H-2^d and H-2^k haplotypes have moderate and weak tumor resistance respectively (Freund et al. 1992). The FVB strain has an H-2^q haplotype, which may be an additional MHC locus that confers susceptibility to polyoma virus induced tumorigenesis. Alternatively, non-MHC genes can also result in a dominant pattern of tumor susceptibility as in the case of the C3H/BiDa strain (Freund et al. 1992).

Strain variations are also relevant to the study of genetic mutations in mouse models of disease. An analysis of targeted disruptions on mammary tumorigenesis in the PyMT model requires breeding of knockout models usually developed in the 129/SvJ-C57Bl/6J background into the FVB background. It is commonly recognized that the FVB strain is susceptible while the C57Bl/6J (B6) strain is more resistant to PyMT mammary tumorigenesis and F1 crosses of these strains increase tumor latency by approximately 6 days (Lifsted et al. 1998). However, it is not clear what effects continued backcrossing has on the analysis of targeted mutations in the PyMT model.

Previously we reported that inducible nitric oxide synthase (iNOS) deficiency in the PyMT model in the B6 background resulted in an increase in tumor latency that was not observed in the FVB background (Ellies et al. 2003). Since the issue of strain background is an important one for analysis of mouse models we have made iNOS

knockout mice congenic in the FVB and B6 backgrounds and carried out a comparison of tumorigenesis and metastasis in both strains.

Materials and methods

Animals

PyMT (FVB/N-Tg(MMTV-PyVT)634Mul/J) mice (Guy et al. 1992) were obtained from W. Muller (McMaster University, Ontario, Canada). We acquired PyMT mice that had been backcrossed 5 generations into the B6 background from A. Varki (UCSD, La Jolla, CA). Control (C57Bl/6J) and iNOS deficient mice (B6.129P2-*Nos2*^{tm1Lau}/J; Laubach et al. 1995) were purchased from The Jackson Laboratory, Bar Harbor, ME. The PyMT B6 mice were further backcrossed until congenic in the B6 background and then bred with iNOS$^{-/-}$ mice. iNOS$^{-/-}$ mice were bred into the FVB background until congenic (>10 generations) and then crossed with PyMT FVB mice. Female mice heterozygous for the PyMT transgene and homozygous for the wild type or mutated iNOS gene were used in these studies. For clarity and brevity, we have designated FVB/N-Tg(MMTV-PyVT) 634Mul/JxB6.129P2-*Nos2*^{tm1Lau}/J$^{+/+}$ mice PyMT/iNOS$^{+/+}$ and FVB/N-Tg(MMTV-PyVT)634Mul/JxB6.129P2-*Nos2*^{tm1Lau}/J$^{-/-}$ mice PyMT/iNOS$^{-/-}$. FVB mice were palpated twice weekly from 4 weeks of age and B6 mice once weekly from 8 weeks of age to monitor mammary tumor development. Tumors were measured in 2 dimensions using calipers and tumor volume estimated using the standard calculation for a sphere $4/3 \times 3.14 \times a \times b^2$ where a is the smaller diameter and b is the larger diameter. After euthanizing the mice, mammary tumors were dissected and weighed and the total tumor burden calculated (tumor weight/body weight). All studies followed the NIH guidelines for the care and treatment of experimental laboratory rodents.

Mammary gland whole mounts

Pairs of inguinal mammary glands were fixed in formalin or Carnoy's fixative, dehydrated through a graded series of ethanol solutions and defatted in xylene. Following rehydration, the mammary epithelium was stained with carmine stain (Sigma Chemical, St Louis, MO) for 30 min. After removing excess stain by washing in water, samples were dehydrated and stored in methyl salicylate (Sigma Chemical, St Louis, MO).

Tumor microvascular density

Cryosections of OCT embedded tumor samples were cut at 7 μm and stained with anti-CD31 clone 13.3 (1:200, BD Pharmingen, San Diego, CA) as previously described (Ellies et al. 2003). Five random fields per tumor were captured on the Spot RT digital camera system (Diagnostic Instruments, Sterling Heights, MI) at 200× magnification and analyzed using the public domain NIH Image program (http://rsb.info.nih.gov/nih-image/). Microvessel areas were normalized to 1 mm^2 of epithelium.

Lung metastases

Paraffin embedded lungs were serial sectioned and stained with hematoxylin and eosin. Both the numbers and areas of lung metastases were measured by light microscopy using images and software from the Spot RT digital camera system. Lung area per section was measured using a dissecting scope and metastatic tumor burden calculated (mm^2 of lung metastases/cm^2 of lung tissue) for each animal using data from 3 sections at least 100 μm apart. At least 13 PyMT/iNOS$^{+/+}$ or PyMT/iNOS$^{-/-}$ mice were used in this analysis.

Statistical analysis

The percentage of mice tumor free in each group was analyzed using a Kaplan-Meier survival analysis, and the log-rank statistic was used for comparison of the curves between groups. The *t*-test was used for comparison of 2 groups and the analysis of variance (ANOVA) followed by the Bonferroni post-test was applied to multiple comparisons. The Mann–Whitney *U* test was used to compare metastastic burden in the PyMT/iNOS$^{+/+}$ and PyMT/iNOS$^{-/-}$ groups.

Results

PyMT tumorigenesis is delayed in the C57Bl/6 strain

The PyMT model was originally developed in the FVB strain due to its high fecundity. Tumor growth occurs rapidly and metastatic tumors form in the lungs (Guy et al. 1992). To compare tumorigenesis in the FVB strain with that in the C57Bl/6 strain onto which many genetically modified strains are bred, we made PyMT mice congenic in the B6 background. Examination of tumor latency showed a dramatic difference with a mean latency of 53 days for PyMT tumor development in FVB mice and 92 days in B6 mice, a delay of approximately 6 weeks (Fig. 1A). Whole mounts of mammary glands from the two strains also showed that even at weaning, hyperplasias were more advanced in FVB than B6 PyMT mice (Fig. 1B).

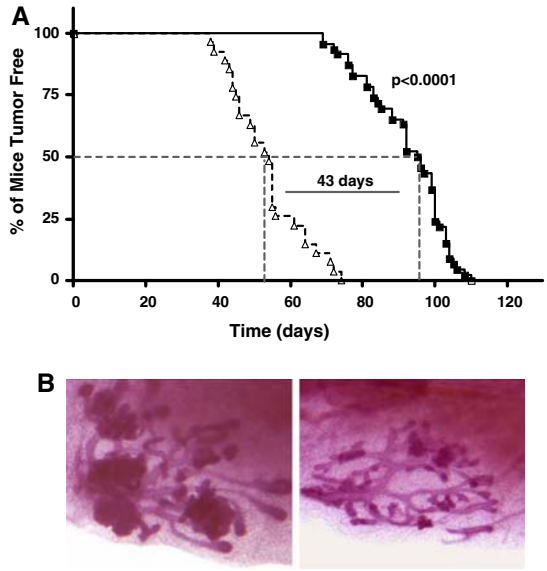

Fig. 1 PyMT tumorigenesis in the FVB and B6 strains. (**A**) The day at which the first mammary tumor was detected by palpation in each mouse was recorded and a Kaplan-Meier survival plot generated. Log rank analysis indicated a highly significant difference, $P < 0.001$ between the curves. -▲- FVB mice $N = 44$, -■-B6 mice $N = 46$. (**B**) Whole mounts of mammary glands from 3 week old PyMT/iNOS$^{+/+}$ mice of the FVB (left panel) and B6 (right panel) strains

Effects of iNOS deficiency are more apparent in the C57Bl/6 background

To determine how this difference in tumor latency may affect the phenotype observed following crossbreeding with genetically altered mice, we bred in iNOS$^{-/-}$ mice congenic in the two backgrounds. As previously reported, we observed a 3–4 week delay in palpable tumors in B6 PyMT mice lacking iNOS activity (Ellies et al. 2003). However, this difference was difficult to discern in the FVB background due to the rapid tumor onset (Fig. 2A). Mammary gland whole mounts reflected the latency data with a clear difference in tumor growth with iNOS deficiency being observed in the #4 glands of B6 PyMT mice (Fig. 2A).

PyMT tumor growth kinetics vary in FVB/N and C57Bl/6 strains

The pattern of tumor growth differed between strains and may in part account for the greater

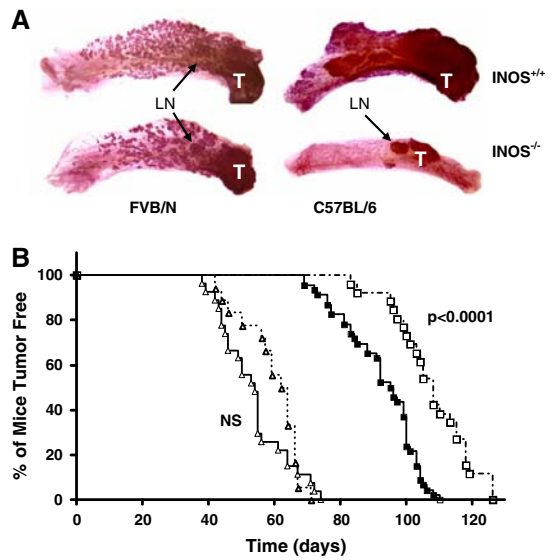

Fig. 2 Effects of iNOS deficiency on mammary tumor development. (**A**) Whole mounts of PyMT/iNOS$^{+/+}$ and PyMT/iNOS$^{-/-}$ #4 mammary glands from 11 week FVB mice or 20 week B6 mice. LN = lymph node. (**B**) Kaplan Meier plots of the tumor latency of PyMT/iNOS$^{+/+}$ annd PyMT/iNOS$^{-/-}$ mice of the 2 strains. Data were analyzed by the log rank test. -▲-PyMT/iNOS$^{+/+}$ FVB $N = 44$, -▲-PyMT/iNOS$^{-/-}$ FVB $N = 57$, -■-PyMT/iNOS$^{+/+}$ B6 $N = 46$, -□-PyMT/iNOS$^{-/-}$ B6 $N = 26$

disparity in tumor development observed in the absence of iNOS in PyMT B6 mice. Once the mean tumor volume reached 1 cm^3, tumor growth proceeded exponentially in the PyMT FVB mice leading to sacrifice within 3 weeks (Fig. 3A). To achieve the same final tumor volume, the PyMT B6 mice required approximately 7 weeks and growth followed a more linear pattern, suggesting more variable rates of growth of individual tumors. Indeed, when we analyzed the tumor latency of all tumors, we were able to define two distinct phases of tumor growth in the B6 strain: early, from 12–17 weeks and late, from 19–23 weeks (Fig. 3B). The major effect of iNOS deficiency appears to be a delay in the early phase of tumor development.

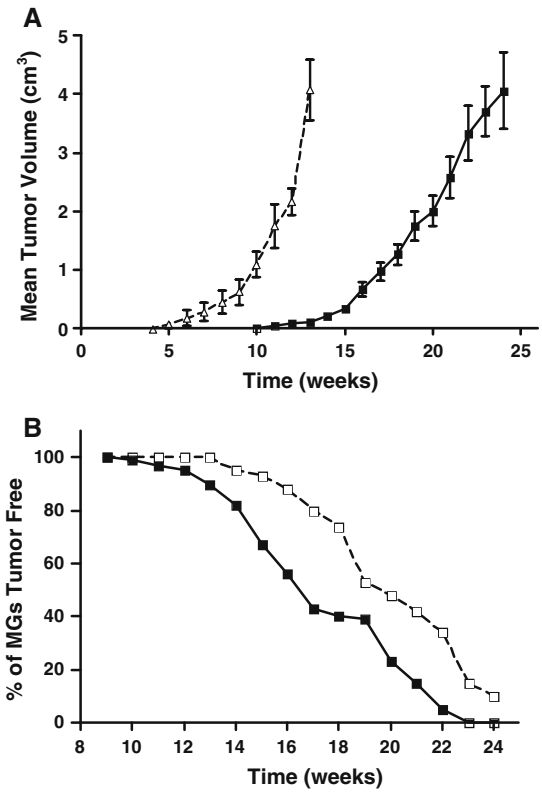

Fig. 3 Mammary tumor growth kinetics. (**A**) Mean tumor volume per mouse. -▲-FVB $N = 32$, -■-B6 $N = 44$. Data are means ± SEM. (**B**) Tumor latency for individual B6 PyMT/iNOS$^{+/+}$ and PyMT/iNOS$^{-/-}$ tumors. Data were derived from examining 460 B6 PyMT/iNOS$^{+/+}$ -■-and 260 PyMT/iNOS$^{-/-}$ -□-tumors

Deficiency in iNOS-modulated tumor growth is site specific

In concordance with increased tumor latency and decreased tumor growth (Ellies et al. 2003) tumor burden was significantly lower in PyMT/iNOS$^{-/-}$ mice (Fig. 4A). An examination of tumor burden in individual mammary glands revealed a reduction in all PyMT/iNOS$^{-/-}$ glands compared to controls, although the numbers were only significant in the #3 and #4 mammary glands (Fig. 4A). It is interesting to note that these are the glands with the largest fat pads and may indicate a role for the stroma in the iNOS effect. To assess a role for tumor vascularization in this effect we examined tumor microvascular density (MVD) in #1and #2–5 tumors of both genotypes. Although there was a slight reduction in the mean MVD in #1 versus #2–5 tumors in the PyMT/iNOS$^{+/+}$ and PyMT/iNOS$^{-/-}$ genotypes, it was not statistically significant, suggesting this is not the mechanism for the difference observed in tumor growth at different locations (Table 1).

This site-specific effect prompted us to examine tumor latency in individual glands. We had observed during palpations that the #1 mammary gland was usually the first to develop tumors, however we were surprised to find a clear difference between the latency of the #1 tumors compared with all other tumors (Fig. 5). This difference was more noticeable in the absence of iNOS. The greater difference in mean latency in the #4 glands compared with the #1 glands was consistent with the tumor burden results being more significant in the #4 glands.

iNOS effects on tumor metastasis

The PyMT model has been useful for the study of tumor metastasis due to the high penetrance of this clinically important characteristic of tumor progression. However, we found that in the FVB strain, tumors were so aggressive that no significant difference could be observed in the metastatic burden occurring in PyMT/iNOS$^{+/+}$ and PyMT/iNOS$^{-/-}$ mice Fig 6. Although the incidence of tumor metastasis was less in the B6 strain, a statistically significant difference between the genotypes was found. We have

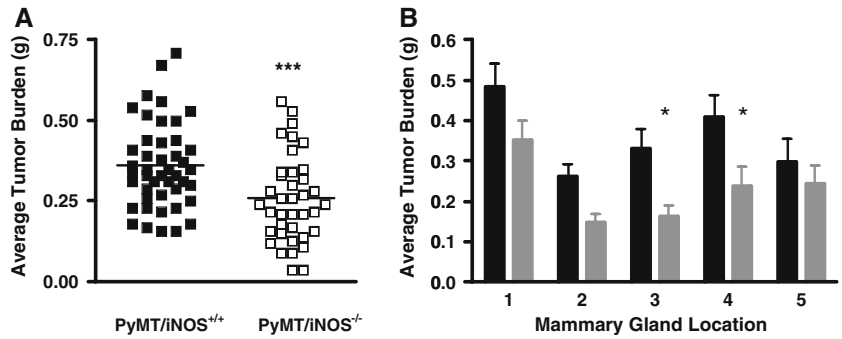

Fig. 4 Distribution of B6 mammary gland tumor burden. (**A**) Total tumor burden was significantly lower in PyMT/iNOS$^{-/-}$ mice, ***$P < 0.001$. (**B**) Examination of individual tumors indicated that a significant difference in genotypes was only found in the #3 and #4 mammary glands, although in each gland the mean tumor burden was lower in PyMT/iNOS$^{-/-}$ mice. *$P < 0.05$ ANOVA followed by Bonferroni post tests. PyMT/iNOS$^{+/+}$ B6 $N = 24$ (black bars), PyMT/iNOS$^{-/-}$ B6 $N = 25$ (grey bars)

maintained PyMT/iNOS$^{-/-}$ mice for up to 32 weeks and found no increase in metastatic burden (data not shown), suggesting that the decrease in metastasis is not due simply to the delayed tumor latency in these mice.

Discussion

Mouse models of mammary tumorigenesis have provided important insights into the molecular basis of human breast cancer and are essential for gathering preclinical data regarding therapeutic drug efficacy. The PyMT model in the FVB strain has a mean tumor latency of 53 days and has been used extensively in studies of mammary tumorigenesis (Cardiff 2003; Muller and Neville 2001). The model is frequently crossed with gene-targeted strains that have been generated in the B6/129 mixed background or backcrossed onto the B6 background. We had highly variable results examining iNOS effects in a mixed B6/FVB PyMT background and sought to characterize

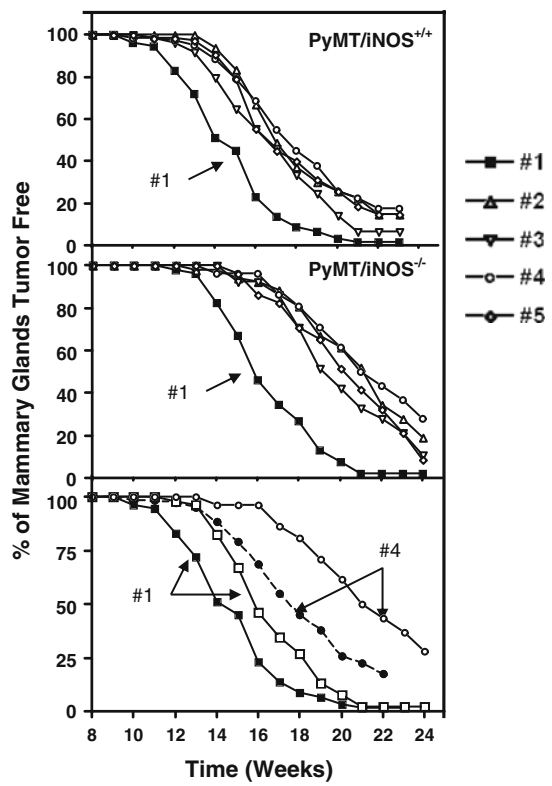

Fig. 5 Tumor latency of individual B6 mammary glands. Tumor latency was lower in the #1 mammary gland in PyMT/iNOS$^{+/+}$ mice compared with all other mammary glands (upper panel). A similar result was observed in PyMT/iNOS$^{+/+}$ mice, with an increase in disparity between the latency of the #1 gland and all other glands (middle panel). When the #1 and #4 latencies for both genotypes were overlayed, a greater difference in mean tumor latency was observed between the #4 glands when compared with the #1 glands (lower panel)

Table 1 Quantitative analysis of tumor microvascular density

Genotype	Location	*N*	MVD ($\mu m^2/mm^2$)
PyMT/iNOS$^{+/+}$	#1	9	216 ± 20
PyMT/iNOS$^{+/+}$	#2–5	9	176 ± 12
PyMT/iNOS$^{-/-}$	#1	6	201 ± 11
PyMT/iNOS$^{-/-}$	#2–5	11	189 ± 11

Data are means ± SEM

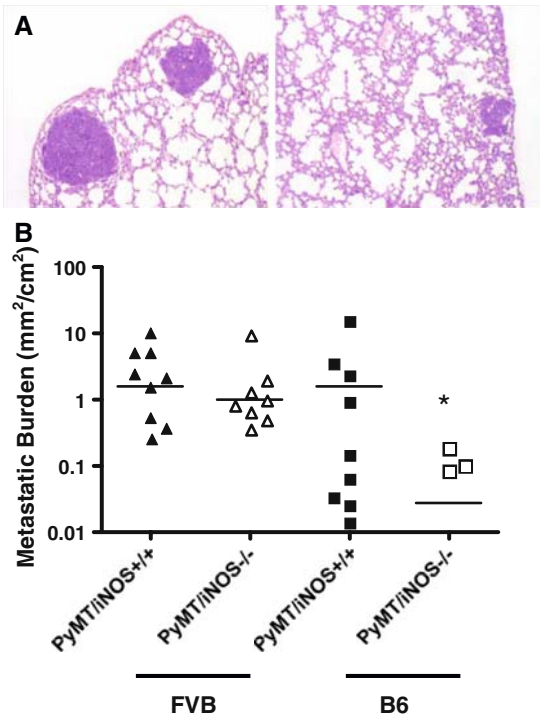

Fig. 6 Tumor metastasis. (**A**) HE stained paraffin embedded sections of PyMT/iNOS$^{+/+}$ (left panel) and PyMT/iNOS$^{-/-}$ (right panel) lungs. (**B**) Comparison of metastatic tumor burden in FVB and B6 mice $^{*}P < 0.05$ Mann-Whitney U test. PyMT/iNOS$^{+/+}$ FVB $N = 14$, PyMT/iNOS$^{-/-}$ FVB $N = 13$, PyMT/iNOS$^{+/+}$ B6 $N = 17$, PyMT/iNOS$^{-/-}$ B6 $N = 21$

the phenotype of this mutation in congenic FVB and B6 strains. Our study demonstrates that the genetic background of the PyMT model can affect the ability to discern differences in phenotype due to genetic alterations that require time to influence tumor progression. Differences observed in the B6 background were obscured in the FVB background due to the signficantly shorter tumor latency and more rapid tumor growth in this strain.

Further analysis of mammary tumorigenesis in the B6 background indicated that tumor formation occurred in 2 phases: early, from 12–17 weeks and late, from 19–23 weeks. It is the early phase of tumor formation that is most affected in the absence of iNOS, consistent with recent data linking iNOS expression with transcriptional upregulation of signal transducers and activators of transcription 3 (STAT3) by nuclear epidermal growth factor receptor (EGFR) (Lo et al. 2005). EGFR/ErbB1, a member of the ErbB family of receptor tyrosine kinases that signal via the same pathways as PyMT (Webster et al. 1998), is also found in the nucleus of highly proliferative cells where is functions as a transcription factor (Marti et al. 1991; Wells and Marti 2002). Structural and functional characterization of the iNOS promoter has identified binding elements for both EGFR and STAT3 (Lo et al. 2005). Immunohistochemical studies of breast carcinomas show that nuclear EGFR positively correlates with iNOS and survival analysis demonstrates that high levels of iNOS are a prognostic indicator of poor survival (Lo et al. 2005). Thus the B6 PyMT mice in the presence or absence of iNOS deficiency are likely to provide an important model for further analysis of these novel molecular interactions.

Mammary tumor latency for each of the ten murine mammary glands has generally been assumed to be stoichiometric. However our data demonstrate that the #1 mammary glands have tumor initiating properties that are distinct from the other 4 pairs of mammary glands. The #1 mammary glands have the smallest fat pads and are located in the head and neck region, which is highly vascular, so we hypothesized that an increase in vascular density in the #1 tumors could be responsible for this difference. An examination of the microvacular density (MVD) of #1 tumors versus all others showed a trend in which #1 tumors had a higher mean MVD than #2–5 tumors as determined by quantitative analysis of CD31 staining. However, these values were not statistically significant, suggesting a different mechanism is responsible for the observed site-specific differences in tumor burden and tumor latency. Other factors in the stromal microevironment may also play a role in mediating this effect. The release of epidermal growth factor (EGF) from the submandibular salivary gland has been shown to promote mouse mammary tumorigenesis in virus mediated and chemical carcinogen induced models (Kurachi et al. 1985; Molinolo et al. 1998). The proximity of the #1 glands to the submandibular gland make EGF induced proliferation a plausible explanation, however further investigations will be required

to determine whether the release of this growth factor primarily affects the #1 glands.

Another possible explanation for this intriguing difference is that the #1 mammary gland is developmentally distinct from the other mammary glands. The #1 gland is not the first to develop since placode 3 develops first at E11.0–11.5 on the ectodermal streak between the forelimb and hindlimb (Eblaghie et al. 2004; Mailleux et al. 2002). Placodes 1 and 5 arise from the axillary and inguinal streaks respectively and placodes 4 and 2 form where the mammary line abuts these streaks (Veltmaat et al. 2004). Recent studies indicate that signaling molecules essential for mammogenesis are placode dependent. Placodes 2 and 3 do not form in the absence of Lef1 mediated canonical Wnt signaling (Boras-Granic et al. 2006) and placodes 1, 2, 3 and 5 require Fgf10 signaling from somites underlying the ectoderm (Mailleux et al. 2002; Veltmaat et al. 2006). It is clear there are developmental differences between mammary glands and it is possible that early developmental factors result in an increased propensity for malignant transformation in the #1 mammary glands, though the identity of these factors remains to be determined.

Since metastasis is an aspect of tumor progression that is critical to patient survival, we examined the effect of iNOS on tumor metastasis in both the FVB and B6 backgrounds. No significant difference in metastatic burden was found in PyMT/iNOS$^{-/-}$ mice in the FVB background, however the tumor burden was reduced in lungs of PyMT/iNOS$^{-/-}$ mice in the B6 background compared with controls. Furthermore, the reduction in metastatic burden was not due simply to the delayed tumor latency as we maintained PyMT/iNOS$^{-/-}$ mice longer to compensate for the difference and found that this did not alter our previous findings (Ellies et al. 2003).

Human clinical studies have associated increased iNOS expression with poor prognosis in breast cancer patients (Loibl et al. 2005), and the use of non-steroidal anti-inflammatory drugs (NSAIDs) with a 22–39% reduction in the risk of breast cancer (Harris et al. 2005; Khuder and Mutgi 2001). To increase our understanding of the molecular pathways involved in these effects, it is essential to have animal models that recapitulate the clinical findings. We have shown that in the PyMT B6 background loss of iNOS, an important inflammatory mediator, results in increased tumor latency and decreased tumor metastasis that is not due simply to the difference in latency. This model will be useful in determining molecular pathways underlying the role of iNOS in breast cancer.

Acknowledgements Drs. Ajit Varki and Lubor Borsig provided the PyMT mice in the C57Bl/6J background. The authors thank the UCSD Cancer Center Histology and Immunohistochemistry Shared Resource for technical assistance. This work was supported by NIH R01-CA81376. L.G.E. was supported by NCI grant K08-CA88035. J.E.M. was a Susan G. Komen Fellow.

References

Boras-Granic K, Chang H, Grosschedl R, Hamel PA (2006) Lef1 is required for the transition of Wnt signaling from mesenchymal to epithelial cells in the mouse embryonic mammary gland. Dev Biol 295:219–231

Cardiff RD (2003) Mouse models of human breast cancer. Comp Med 53:250–253

Cardiff RD, Wellings SR (1999) The comparative pathology of human and mouse mammary glands. J Mammary Gland Biol Neoplasia 4:105–122

Eblaghie MC, Song SJ, Kim JY, Akita K, Tickle C, Jung HS (2004) Interactions between FGF and Wnt signals and Tbx3 gene expression in mammary gland initiation in mouse embryos. J Anat 205:1–13

Ellies LG, Fishman M, Hardison J, Kleeman J, Maglione J, Manner CK, Cardiff RD, MacLeod CL (2003) Mammary tumor latency is increased in mice lacking the inducible nitric oxide synthase. Int J Cancer 106:1–7

Fargiano AA, Desai KV, Green JE (2003) Interrogating mouse mammary cancer models: insights from gene expression profiling. J Mammary Gland Biol Neoplasia 8:321–334

Freund R, Dubensky T, Bronson R, Sotnikov A, Carroll J, Benjamin T (1992) Polyoma tumorigenesis in mice: evidence for dominant resistance and dominant susceptibility genes of the host. Virology 191:724–731

Gross LG (1983). Oncogenic Viruses, 3rd edn. Oxford, Pergamon Press

Guy C, Cardiff R, Muller W (1992) Induction of mammary tumors by expression of polyomavirus middle T oncogene: a transgenic mouse model for metastatic disease. Mol Cell Biol 12:954–961

Guy C, Muthuswamy S, Cardiff R, Soriano P, Muller W (1994) Activation of the c-Src tyrosine kinase is required for the induction of mammary tumors in transgenic mice. Genes Dev 8:23–32

Harris RE, Beebe-Donk J, Doss H, Burr Doss D (2005) Aspirin, ibuprofen, and other non-steroidal anti-

inflammatory drugs in cancer prevention: a critical review of non-selective COX-2 blockade. Oncol Rep 13:559–583

Khuder SA, Mutgi AB (2001) Breast cancer and NSAID use: a meta-analysis. Br J Cancer 84:1188–1192

Kurachi H, Okamoto S, Oka T (1985) Evidence for the involvement of the submandibular gland epidermal growth factor in mouse mammary tumorigenesis. Proc Natl Acad Sci USA 82:5940–5943

Laubach V, Shesely E, Smithies O, Sherman P (1995) Mice lacking inducible nitric oxide synthase are not resistant to lipopolysaccharide-induced death. PNAS, USA 92:10688–10692

Law LW, Ting RC, Leckband E (1967) Prevention of virus-induced neoplasms in mice through passive transfer of immunity by sensitized syngeneic lymphoid cells. Proc Natl Acad Sci USA 57:1068–1075

Le Voyer T, Lu Z, Babb J, Lifsted T, Williams M, Hunter K (2000) An epistatic interaction controls the latency of a transgene-induced mammary tumor. Mamm Genome 11:883–889

Lifsted T, Le Voyer T, Williams M, Muller W, Klein-Szanto A, Buetow KH, Hunter KW (1998) Identification of inbred mouse strains harboring genetic modifiers of mammary tumor age of onset and metastatic progression. Int J Cancer 77:640–644

Lin EY, Nguyen AV, Russell RG, Pollard JW (2001) Colony-stimulating factor 1 promotes progression of mammary tumors to malignancy. J Exp Med 193:727–740

Lo HW, Hsu SC, Ali-Seyed M, Gunduz M, Xia W, Wei Y, Bartholomeusz G, Shih JY, Hung MC (2005) Nuclear interaction of EGFR and STAT3 in the activation of the iNOS/NO pathway. Cancer Cell 7:575–589

Loibl S, Buck A, Strank C, von Minckwitz G, Roller M, Sinn HP, Schini-Kerth V, Solbach C, Strebhardt K, Kaufmann M (2005) The role of early expression of inducible nitric oxide synthase in human breast cancer. Eur J Cancer 41:265–271

Ma XJ, Salunga R, Tuggle JT, Gaudet J, Enright E, McQuary P, Payette T, Pistone M, Stecker K, Zhang BM, et al. (2003) Gene expression profiles of human breast cancer progression. Proc Natl Acad Sci USA 100:5974–5979

Mailleux AA, Spencer-Dene B, Dillon C, Ndiaye D, Savona-Baron C, Itoh N, Kato S, Dickson C, Thiery JP, Bellusci S (2002) Role of FGF10/FGFR2b signaling during mammary gland development in the mouse embryo. Development 129:53–60

Marti U, Burwen SJ, Wells A, Barker ME, Huling S, Feren AM, Jones AL (1991) Localization of epidermal growth factor receptor in hepatocyte nuclei. Hepatology 13:15–20

Molinolo A, Simian M, Vanzulli S, Pazos P, Lamb C, Montecchia F, Lanari C (1998). Involvement of EGF in medroxyprogesterone acetate (MPA)-induced mammary gland hyperplasia and its role in MPA-induced mammary tumors in BALB/c mice. Cancer Lett 126:49–57

Muller WJ, Neville MC (2001) Introduction: Signaling in mammary development and tumorigenesis. J Mammary Gland Biol Neoplasia 6:1–5

Qiu TH, Chandramouli GV, Hunter KW, Alkharouf NW, Green JE, Liu ET (2004) Global expression profiling identifies signatures of tumor virulence in MMTV-PyMT-transgenic mice: correlation to human disease. Cancer Res 64:5973–5981

Ramaswamy S, Ross KN, Lander ES, Golub TR (2003) A molecular signature of metastasis in primary solid tumors. Nat Genet 33:49–54

Rosner A, Miyoshi K, Landesman-Bollag E, Xu X, Seldin DC, Moser AR, MacLeod CL, Shyamala G, Gillgrass AE, Cardiff RD (2002) Pathway pathology: histological differences between ErbB/Ras and Wnt pathway transgenic mammary tumors. Am J Pathol 161:1087–1097

Ting RC, Law LW (1965) The role of thymus in transplantation resistance induced by polyoma virus. J Natl Cancer Inst 34:521–527

Veltmaat JM, Relaix F, Le LT, Kratochwil K, Sala FG, van Veelen W, Rice R, Spencer-Dene B, Mailleux AA, Rice DP, et al. (2006) Gli3-mediated somitic Fgf10 expression gradients are required for the induction and patterning of mammary epithelium along the embryonic axes. Development 133:2325–2335

Veltmaat JM, Van Veelen W, Thiery JP, Bellusci S (2004) Identification of the mammary line in mouse by Wnt10b expression. Dev Dyn 229:349–356

Webster MA, Hutchinson JN, Rauh MJ, Muthuswamy SK, Anton M, Tortorice CG, Cardiff RD, Graham FL, Hassell JA, Muller WJ (1998) Requirement for both Shc and phosphatidylinositol 3′ kinase signaling pathways in polyomavirus middle T-mediated mammary tumorigenesis. Mol Cell Biol 18:2344–2359

Wells A, Marti U (2002) Signalling shortcuts: cell-surface receptors in the nucleus? Nat Rev Mol Cell Biol 3:697–702

Williams TM, Medina F, Badano I, Hazan RB, Hutchinson J, Muller WJ, Chopra NG, Scherer PE, Pestell RG, Lisanti MP (2004) Caveolin-1 gene disruption promotes mammary tumorigenesis and dramatically enhances lung metastasis in vivo. Role of Cav-1 in cell invasiveness and matrix metalloproteinase (MMP-2/9) secretion. J Biol Chem 279:51630–51646